The infrared emission spectra of LiF and HF

H. G. HEDDERICH,[1] C. I. FRUM, R. ENGLEMAN, JR., AND P. F. BERNATH[1]
Department of Chemistry, The University of Arizona, Tucson, AZ 85721, U.S.A.

Received March 20, 1991

This paper is dedicated to Dr. Richard Norman Jones

H. G. HEDDERICH, C. I. FRUM, R. ENGLEMAN, JR., and P. F. BERNATH. Can. J. Chem. **69**, 1659 (1991).

The high resolution infrared spectrum of LiF has been measured in emission with the McMath Fourier transform interferometer at Kitt Peak. A total of 800 lines with $v = 1 \rightarrow 0$ to $v = 8 \rightarrow 7$ of the main isotopomer, ^{7}LiF, and 250 lines with $v = 1 \rightarrow 0$ to $v = 3 \rightarrow 2$ of the minor isotopomer, ^{6}LiF, were observed. These ro-vibrational transitions and the pure rotational transitions from the literature were fit to a set of Dunham coefficients Y_{ij} and a set of mass-reduced Dunham coefficients U_{ij}. The same spectrum shows 13 pure rotational emission transitions of HF in the vibrational ground state with $J = 13 \rightarrow 12$ to $J = 25 \rightarrow 24$. These transitions were used to determine an improved set of rotational constants for HF.

Key words: infrared spectra, LiF, HF.

H. G. HEDDERICH, C. I. FRUM, R. ENGLEMAN, JR. et P. F. BERNATH. Can. J. Chem. **69**, 1659 (1991).

On a mesuré les spectres d'émission infrarouge à haute résolution du LiF à l'aide d'un interféromètre à transformation de McMath Fourier au niveau Kitt Peak. On a observé 800 raies avec des valeurs de v allant de $v = 1 \rightarrow 0$ à $v = 8 \rightarrow 7$ pour l'isotopomère principal, ^{7}LiF, et on a observé 250 raies avec des valeurs de v allant de $v = 1 \rightarrow 0$ à $v = 8 \rightarrow 7$ pour l'isotopomère minoritaire. On a adapté ces transitions de vibration-ro et les transitions de rotation pure répertoriées dans la littérature à un ensemble de coefficients de Dunham Y_{ij} et à un ensemble de coefficients U_{ij} de masse réduite Dunham. Ces mêmes spectres montrent 13 transitions d'émission de rotation pure du HF dans l'état fondamental de vibration avec $J = 13 \rightarrow 12$ à $J = 25 \rightarrow 24$. On a utilisé ces transitions pour déterminer un ensemble amélioré de constantes de rotation pour le HF.

Mots clés : spectres infrarouge, LiF, HF.

[Traduit par la rédaction]

I. Introduction

The infrared spectra of alkali halides have been of interest to spectroscopists for a long time (1, 2). However, high-resolution infrared data for these molecules have only become available after the introduction of diode laser and Fourier transform infrared spectrometers. Nevertheless, the first infrared data on LiF was obtained by Vidale (3) as early as 1959 with a Perkin-Elmer grating spectrometer. He observed the spectrum of LiF both in absorption and emission. However, the resolution was not high enough to obtain an unambiguous rotational assignment and, therefore, the correct band center. Vidale gave three possible assignments. Only after the microwave measurements on ^{6}LiF by Wharton *et al.* (4) did the correct assignment become apparent. Several additional papers report the infrared spectrum of LiF trapped in low temperature matrices (5–10).

The first high-resolution infrared data on LiF was published by Maki (11). He used a tunable diode laser system for the observation of ro-vibrational transitions with $v = 1 \leftarrow 0$ to $v = 8 \leftarrow 7$ for ^{7}LiF and ^{6}LiF. Diode lasers display many gaps in their spectral coverage. Therefore, only a few lines of each vibrational band were accessible. In this paper the complete emission spectra of ^{7}LiF and ^{6}LiF between 630 and 1030 cm^{-1} are published (Figs. 1, 2).

HF is an important gas for use as an absolute wavenumber standard. In 1987 Jennings *et al.* (12) published rotational constants for HF calculated from measurements in four different laboratories. Highly accurate data in the far infrared ($J = 1 \leftarrow 0$ to $J = 4 \leftarrow 3$) were obtained with a tunable far-infrared spectrometer at the National Bureau of Standards laboratory in Boulder. Transitions with $J = 5 \leftarrow 4$ to $J = 7 \leftarrow 6$ were measured with a commercial high-resolution Fourier transform spectrometer at the National Research Council, Ottawa, Canada. Lines with $J = 17$ to $J = 21$ were observed with a vacuum grating spectrograph (13) and lines with $J = 26$ to $J = 32$ with a tunable diode laser spectrometer at the University of Lille, France. In 1988 Jennings and Wells (14) remeasured the $J = 27 \leftarrow 26$ and $J = 33 \leftarrow 32$ transitions by using a tunable diode laser heterodyne spectrometer (15). Except for these two lines, the mid-infrared transitions are relatively inaccurate. Unfortunately the uncertainties in the molecular constants in this publication seem to be a factor of 10 too small. As a by-product of our work with LiF, we publish thirteen rotational transitions of HF in the range 500 to 900 cm^{-1}. A new fit including the far-infrared data and the diode laser measurements provide an improved set of rotational constants for HF.

II. Experimental

The high resolution infrared emission spectra of ^{6}LiF, ^{7}LiF, and HF between 500 and 1400 cm^{-1} were observed with the McMath Fourier transform spectrometer at Kitt Peak. The unapodized resolution was 0.0055 cm^{-1} with a liquid helium cooled As:Si detector and a KCl beamsplitter. The upper wavenumber limit was set by a wedged InSb filter while the lower limit was given by the transmission of the KCl beamsplitter and by the detector response. The spectrum of LiF was taken accidentally during an attempt to observe the infrared spectrum of MgF_2.

Solid MgF_2 was heated to about 1500 K in an alumina tube furnace. The apparatus used for the experiment was described in detail earlier (16). The heating rate was about 5 K/min. The temperature of the furnace was measured with a chromel–alumel thermocouple placed between the heating elements and the alumina tube. Deposition of solid material onto the windows was avoided by pressurizing the cell with 5 Torr of argon. A series of spectra were taken as the furnace heated up and then cooled down. Initially a globar was placed behind the tube furnace and its image was focused on the 8 mm aperture of the Fourier transform spectrometer. No absorption spectra were observed, but when the globar was shut off (at a temperature of about 1300 K) an emission spectrum was monitored. The inten-

[1]Also affiliated with Centre for Molecular Beams and Laser Chemistry, Department of Chemistry, The University of Waterloo, Waterloo, Ont., Canada N2L 3G1.

Printed in Canada / Imprimé au Canada

TABLE 1. Ro-vibrational transitions of ^{7}LiF and ^{6}LiF

	J''	Obs./cm^{-1}	Obs. − calc. /10^{-5} cm^{-1}
^{7}LiF			
v = 1→0	P67	643.22499(50)[a]	−32
	P66	647.79186(50)	−14
	P65	652.34367(100)	11
	P64	656.87691(50)	3
	P63	661.39365(50)	5
	P62	665.89322(50)	21
	P61	670.37521(50)	56
	P60	674.83778(50)	−20
	P59	679.28310(50)	52
	P58	683.70808(50)	60
	P57	688.11522(150)	130
	P56	692.49965(50)	−11
	P55	696.86537(50)	1
	P54	701.21006(50)	22
	P53	705.53328(50)	5
	P52	709.83535(50)	38
	P51	714.11486(50)	21
	P50	718.37200(50)	12
	P49	722.60630(50)	6
	P48	726.81744(50)	10
	P47	731.00488(50)	10
	P46	735.16819(50)	2
	P45	739.30720(50)	9
	P44	743.42133(50)	12
	P43	747.51018(50)	9
	P42	751.57345(50)	10
	P41	755.61069(50)	7
	P40	759.62154(50)	3
	P39	763.60582(50)	18
	P38	767.56266(50)	1
	P37	771.49217(50)	3
	P36	775.39382(50)	6
	P35	779.26714(50)	1
	P34	783.11189(50)	1
	P33	786.92762(50)	−4
	P32	790.71410(50)	1
	P31	794.47076(50)	−5
	P30	798.19745(50)	−3
	P29	801.89368(50)	−4
	P28	805.55917(50)	−3
	P27	809.19351(50)	−5
	P26	812.79639(50)	−5
	P25	816.36742(50)	−9
	P24	819.90638(50)	−4
	P23	823.41278(50)	−5
	P22	826.88635(50)	−4
	P21	830.32668(50)	−10
	P20	833.73363(50)	−3
	P19	837.10660(50)	−9
	P18	840.44548(50)	−8
	P17	843.74986(50)	−6
	P16	847.01934(50)	−11
	P15	850.25377(50)	−7
	P14	853.45267(50)	−10
	P13	856.61580(50)	−11
	P12	859.74286(50)	−9
	P11	862.83347(50)	−11
	P10	865.88735(50)	−14
	P9	868.90424(50)	−14
	P8	871.88380(50)	−13
	P7	874.82572(50)	−13
	P6	877.73041(50)	57
	P5	880.59549(50)	−11
	P4	883.42268(50)	−16
	P3	886.21112(50)	−15
	P2	888.96043(50)	−16
	P1	891.67033(50)	−19
	R0	896.97099(50)	−10
	R1	899.56097(50)	−19
	R2	902.11051(50)	−23
	R3	904.61936(50)	−17
	R4	907.08707(50)	−21
	R5	909.51355(50)	−17
	R6	911.89840(50)	−18
	R7	914.24140(50)	−20
	R8	916.54237(50)	−16
	R10	921.01692(50)	−16
	R11	923.19005(50)	−16
	R12	925.32007(50)	−17
	R13	927.40677(50)	−17
	R14	929.44992(50)	−13
	R15	931.44921(50)	−14
	R16	933.40445(50)	−16
	R17	935.31541(50)	−18
	R18	937.18186(50)	−20
	R19	939.00368(50)	−12
	R20	940.78049(50)	−11
	R21	942.51208(50)	−16
	R22	944.19838(50)	−11
	R23	945.83905(50)	−11
	R24	947.43398(50)	−5
	R25	948.98282(50)	−9
	R26	950.48550(50)	−8
	R27	851.94180(50)	−7
	R28	953.35151(50)	−5
	R29	954.71447(50)	−1
	R30	956.03041(50)	−3
	R31	957.29927(50)	1
	R32	958.52075(50)	−1
	R33	959.69477(50)	1
	R34	960.82113(50)	3
	R35	961.89967(50)	6
	R36	962.93020(50)	8
	R37	963.91257(50)	9
	R38	964.84670(50)	16
	R39	965.73172(50)	−42
	R40	966.56926(50)	13
	R41	967.35751(50)	13
	R42	968.09690(50)	16
	R43	968.78722(50)	14
	R44	969.42838(50)	10
	R45	970.02040(50)	20
	R46	970.56296(50)	23
	R47	971.05594(50)	19
	R48	971.49941(50)	27
	R49	971.89296(50)	16
	R50	972.23690(50)	27
	R51	972.53012(50)	−41
	R52	972.77459(50)	20
	R53	972.96841(50)	26
	R54	973.11156(50)	−14
	R55	973.20486(50)	−11
	R58	973.18288(50)	−9
	R59	973.07410(50)	28
	R60	972.91472(50)	5
	R61	972.70458(50)	−28
	R62	972.44380(100)	−56

TABLE 1 (*continued*)

	J''	Obs./cm^{-1}	Obs. − calc. /10^{-5} cm^{-1}		J''	Obs./cm^{-1}	Obs. − calc. /10^{-5} cm^{-1}
	R63	972.13208(100)	−103		P4	867.67416(50)	−17
	R64	971.76979(150)	−131		P3	870.42072(50)	−25
	R66	970.88707(1000)	−757		P2	873.12879(50)	−32
	R67	631.22869(50)	−31		P1	875.79864(50)	17
$v = 2 \rightarrow 1$	P66	635.72007(50)	−54		R0	881.01967(50)	−9
	P65	640.19664(50)	12		R1	883.57101(50)	−11
	P64	644.65580(50)	−49		R2	886.08249(50)	−11
	P63	649.09925(50)	−24		R3	888.55365(50)	−28
	P62	653.52568(50)	−2		R4	890.98463(50)	−21
	P61	657.93478(50)	30		R5	893.37488(50)	−19
	P60	662.32515(50)	−27		R6	895.72416(50)	−20
	P59	666.69846(50)	30		R7	898.03226(50)	−19
	P58	671.05195(50)	−10		R8	900.29890(50)	−19
	P57	675.38687(50)	−4		R9	902.52385(50)	−17
	P56	679.70218(50)	−7		R10	904.70683(50)	−17
	P55	683.99744(50)	−21		R11	906.84760(50)	−18
	P54	688.27260(50)	−9		R12	908.94670(50)	59
	P53	692.52716(50)	18		R13	911.00160(50)	−16
	P52	696.76022(50)	12		R14	913.01435(50)	−15
	P51	700.97172(50)	6		R15	914.98392(50)	−16
	P50	705.16135(50)	11		R16	916.91013(50)	−15
	P49	709.32807(50)	−39		R18	920.63150(50)	−13
	P48	713.47301(50)	10		R19	922.42624(50)	−10
	P47	717.59424(50)	4		R20	924.17663(50)	−16
	P46	721.69209(50)	16		R21	925.88263(50)	−12
	P45	725.76575(50)	3		R22	927.54388(50)	−13
	P44	729.81524(50)	6		R23	929.16031(50)	−7
	P43	733.83991(50)	−1		R24	930.73159(50)	−6
	P42	737.83964(50)	8		R25	932.25754(50)	−8
	P41	741.81377(50)	5		R26	933.73800(50)	−9
	P40	745.76208(50)	7		R27	935.17279(50)	−8
	P39	749.68415(50)	7		R28	936.56172(50)	−5
	P38	753.57956(50)	3		R29	937.90461(50)	1
	P37	757.44812(50)	13		R30	939.20117(50)	−2
	P36	761.28913(50)	2		R31	940.45135(50)	−1
	P35	765.10256(50)	5		R32	941.65492(50)	0
	P34	768.88784(50)	2		R33	942.81174(50)	2
	P33	772.64482(50)	14		R34	943.92159(50)	0
	P32	776.37275(50)	1		R35	944.98457(50)	21
	P31	780.07159(50)	−4		R36	945.99995(50)	8
	P29	787.38047(50)	−3		R37	946.96804(50)	7
	P28	790.98979(50)	1		R38	947.88866(50)	15
	P27	794.56839(50)	−9		R39	948.76142(50)	8
	P26	798.11622(50)	−4		R40	949.58641(50)	9
	P25	801.63268(50)	−9		R41	950.36345(50)	14
	P24	805.11760(50)	−8		R42	951.09230(50)	12
	P23	808.57063(50)	−2		R43	951.77288(50)	9
	P22	811.99123(50)	−10		R44	952.40513(50)	11
	P21	815.37936(50)	−4		R45	952.98891(50)	15
	P20	818.73443(50)	−9		R46	953.52413(50)	26
	P19	822.05627(50)	−10		R47	954.01031(50)	5
	P18	825.34455(50)	−6		R48	954.44802(50)	21
	P17	828.59880(50)	−12		R49	954.83642(50)	1
	P16	831.81897(50)	−1		R50	955.17610(50)	12
	P15	835.00440(50)	−8		R51	955.46643(50)	2
	P13	841.27036(50)	−12		R52	955.70813(100)	52
	P12	844.35032(50)	−5		R53	955.89976(50)	26
	P11	847.39426(50)	−17		R55	956.13526(50)	22
	P10	850.40221(50)	−15		R58	956.11660(50)	−6
	P9	853.37365(50)	−21		R60	955.85520(100)	−71
	P8	856.30845(50)	−17		R61	955.65116(50)	32
	P7	859.20616(50)	−18		R62	955.39582(50)	−8
	P6	862.06649(50)	−24		R63	955.09177(50)	69
	P5	864.88929(50)	−20	$v = 3 \rightarrow 2$	P63	637.08050(50)	47

TABLE 1 (*continued*)

	J''	Obs./cm^{-1}	Obs. − calc. /10^{-5} cm^{-1}
	P62	641.43448(50)	38
	P61	645.77142(50)	23
	P60	650.09061(50)	−26
	P59	654.39259(50)	−14
	P58	658.67705(50)	71
	P57	662.94016(100)	−114
	P56	667.18712(50)	−7
	P55	671.41350(50)	−10
	P54	675.62027(50)	14
	P53	679.80640(50)	4
	P52	683.97197(50)	6
	P51	688.11522(100)	−114
	P50	692.23944(50)	12
	P49	696.34045(50)	7
	P48	700.41927(50)	10
	P47	704.47535(50)	7
	P46	708.50834(50)	1
	P45	712.51815(50)	23
	P44	716.50367(50)	−1
	P43	720.46523(50)	1
	P42	724.40076(150)	−140
	P41	728.31423(50)	11
	P40	732.20075(50)	2
	P39	736.06160(50)	−1
	P38	739.89648(50)	9
	P37	743.70475(50)	4
	P36	747.48629(50)	11
	P35	751.24050(50)	4
	P34	754.96726(50)	8
	P33	758.66554(50)	−44
	P32	762.33658(50)	9
	P31	765.97844(50)	7
	P30	769.59128(50)	1
	P29	773.17489(50)	7
	P28	776.72871(50)	3
	P27	780.25263(50)	11
	P25	787.20868(50)	−3
	P24	790.64043(50)	4
	P23	794.04065(50)	−2
	P22	797.40920(50)	−3
	P21	800.74569(50)	−3
	P20	804.04978(50)	−4
	P19	807.32117(50)	−4
	P18	810.55952(50)	−4
	P17	813.76451(50)	−3
	P16	816.93581(50)	−3
	P15	820.07305(50)	−8
	P14	823.17607(50)	−5
	P13	826.24442(50)	−5
	P12	829.27779(50)	−10
	P11	832.27601(50)	−5
	P10	835.23860(50)	−9
	P8	841.05602(50)	−7
	P7	843.91016(50)	−11
	P6	846.72833(100)	62
	P5	849.50808(50)	−4
	P4	852.25109(50)	−11
	P3	854.95662(50)	−6
	P2	857.62348(100)	−79
	P1	860.25368(50)	−1
	R0	865.39691(50)	−1
	R1	867.90996(50)	−21
	R2	870.38398(50)	−18
	R3	872.81853(50)	−10
	R4	875.21320(50)	−9
	R5	877.56817(50)	27
	R6	879.88235(50)	15
	R7	882.15584(50)	−10
	R8	884.38874(50)	−11
	R9	886.58060(50)	−10
	R10	888.73113(50)	−10
	R11	890.84013(50)	−8
	R12	892.90734(50)	−6
	R13	894.93247(50)	−8
	R14	896.91535(50)	−9
	R15	898.85576(50)	−7
	R16	900.75346(50)	−5
	R17	902.60817(50)	−6
	R18	904.41976(50)	−4
	R19	906.18792(50)	−6
	R20	907.91254(50)	−3
	R21	909.59335(50)	0
	R22	911.23010(50)	−2
	R23	912.82266(50)	−2
	R24	914.37083(50)	1
	R25	915.87433(50)	−2
	R26	917.33306(50)	−1
	R27	918.74679(50)	−2
	R28	920.11539(50)	3
	R29	921.43861(50)	5
	R30	922.71629(50)	7
	R31	923.94823(50)	7
	R32	925.13427(50)	5
	R33	926.27433(50)	10
	R34	927.36815(50)	12
	R35	928.41551(50)	5
	R36	929.41649(50)	12
	R37	930.37073(50)	14
	R38	931.27823(50)	24
	R39	932.13854(50)	12
	R40	932.95179(50)	4
	R41	933.71793(50)	9
	R42	934.43673(50)	18
	R43	935.10785(50)	8
	R44	935.73142(50)	6
	R45	936.30716(50)	−6
	R46	936.83529(50)	6
	R47	937.31524(50)	−4
	R48	937.74720(50)	−7
	R49	938.13106(50)	−3
	R50	938.46692(50)	26
	R51	938.75398(50)	11
	R54	939.32502(50)	44
	R55	939.41816(100)	58
	R58	939.40280(100)	−116
$v = 4 \rightarrow 3$	P61	633.87765(50)	−1
	P60	638.12641(100)	−83
	P59	642.35907(50)	−35
	P58	646.57356(50)	−25
	P57	650.76959(50)	−38
	P56	654.94728(50)	−24
	P55	659.10622(50)	19
	P54	663.24355(150)	−156
	P53	667.36412(50)	−24
	P52	671.46338(50)	1
	P51	675.54147(50)	−27
	P50	679.59883(50)	−27
	P49	683.63493(50)	−10

TABLE 1 (*continued*)

	J''	Obs./cm^{-1}	Obs. − calc. /10^{-5} cm^{-1}
	P48	687.64923(50)	8
	P47	691.64100(50)	−7
	P46	695.61031(50)	−9
	P45	699.55677(50)	1
	P44	703.47971(50)	−7
	P43	707.37895(50)	−11
	P42	711.25435(50)	12
	P41	715.10502(50)	10
	P40	718.93082(50)	7
	P39	722.73143(50)	8
	P38	726.50642(50)	7
	P37	730.25548(50)	8
	P36	733.97812(50)	1
	P35	737.67426(50)	13
	P34	741.34315(50)	4
	P33	744.98473(50)	5
	P32	748.59889(50)	40
	P31	752.18426(50)	7
	P30	755.74152(50)	10
	P28	762.76918(50)	8
	P27	766.23995(100)	110
	P26	769.67877(50)	0
	P25	773.08856(50)	6
	P24	776.46786(50)	14
	P23	779.81612(50)	4
	P22	783.13355(50)	29
	P21	786.41897(50)	4
	P20	789.67280(50)	4
	P19	792.89451(50)	9
	P18	796.08353(50)	−6
	P17	799.23978(50)	−18
	P16	802.36319(50)	−2
	P15	805.45303(50)	1
	P14	808.50912(50)	4
	P13	811.53103(50)	−5
	P12	814.51865(50)	−6
	P11	817.47133(50)	−35
	P10	820.38974(50)	7
	P9	823.27215(50)	−24
	P8	826.11958(50)	4
	P7	828.93075(50)	−8
	P6	831.70600(50)	3
	P5	834.44486(50)	19
	P4	837.14646(50)	−17
	P3	839.81170(50)	11
	P2	842.43925(50)	0
	P1	845.02984(50)	49
	R0	850.09554(50)	−19
	R1	852.57155(50)	7
	R2	855.00854(50)	−3
	R3	857.40662(50)	−14
	R4	859.76600(50)	24
	R5	862.08542(50)	9
	R6	864.36526(50)	5
	R7	866.60519(50)	4
	R8	868.80486(50)	−5
	R9	870.96427(50)	5
	R10	873.08284(50)	−2
	R11	875.16049(50)	−10
	R12	877.19718(50)	2
	R13	879.19241(50)	7
	R15	883.05771(50)	8
	R16	884.92738(50)	9
	R17	886.75478(50)	12
	R18	888.53957(50)	4
	R19	890.28173(50)	6
	R20	891.98095(50)	6
	R21	893.63709(50)	11
	R22	895.24986(50)	13
	R23	896.81903(50)	9
	R24	898.34452(50)	11
	R25	899.82602(50)	6
	R26	901.26345(50)	6
	R27	902.65654(50)	3
	R28	904.00516(50)	0
	R29	905.30926(50)	12
	R30	906.56825(50)	−3
	R31	907.78243(50)	2
	R33	910.07504(50)	5
	R34	911.15319(50)	8
	R35	912.18567(50)	9
	R36	913.17222(50)	−2
	R37	914.11269(50)	−26
	R38	915.00775(50)	19
	R39	915.85593(50)	−1
	R40	916.65813(50)	19
	R41	917.41343(50)	−2
	R42	918.12241(50)	9
	R44	919.40004(50)	34
	R45	919.96811(50)	14
	R46	920.48895(50)	−20
	R47	920.96316(50)	3
	R48	921.39014(50)	34
	R49	921.76922(50)	13
	R50	922.10129(50)	41
	R52	922.62144(50)	−22
	R54	922.95179(50)	29
$v = 5 \rightarrow 4$	P57	638.86621(50)	31
	P56	642.97601(50)	−20
	P55	647.06761(50)	−31
	P54	651.14147(100)	84
	P53	655.19459(50)	64
	P52	659.22747(50)	−2
	P51	663.24355(300)	271
	P50	667.23339(50)	−22
	P49	671.20542(50)	−1
	P48	675.15624(50)	35
	P47	679.08464(50)	3
	P46	682.99066(100)	−56
	P45	686.87564(50)	31
	P44	690.73652(50)	−3
	P43	694.57445(50)	−8
	P42	698.38898(50)	11
	P41	702.17991(100)	70
	P40	705.94515(50)	−3
	P39	709.68645(50)	4
	P38	713.40242(50)	−12
	P37	717.09308(50)	−12
	P36	720.75821(50)	19
	P34	728.00889(50)	13
	P33	731.59387(50)	−8
	P32	735.15166(50)	−24
	P31	738.68227(50)	3
	P30	742.18469(50)	6
	P29	745.65885(50)	12
	P28	749.10425(50)	6
	P27	752.52062(50)	−5
	P26	755.90785(50)	1

TABLE 1 (*continued*)

	J''	Obs./cm^{-1}	Obs. − calc. /10^{-5} cm^{-1}
	P24	762.59288(50)	1
	P23	765.89020(50)	12
	P22	769.15714(50)	5
	P21	772.39227(50)	4
	P20	775.59618(50)	−34
	P29	778.76916(50)	−3
	P18	781.90999(50)	6
	P17	785.01842(50)	2
	P16	788.09442(50)	11
	P15	791.13745(50)	11
	P14	794.14719(50)	2
	P13	797.12355(50)	4
	P12	800.06611(50)	6
	P11	802.97466(50)	18
	P10	805.84856(50)	5
	P9	808.68758(50)	−26
	P8	811.49219(50)	2
	P6	816.99486(50)	15
	P5	819.69328(100)	95
	P4	822.35384(50)	3
	P3	824.98004(150)	118
	P2	827.56823(100)	101
	R1	837.54801(50)	−17
	R2	839.94955(50)	58
	R3	842.31126(50)	−19
	R4	844.63543(50)	6
	R5	846.92047(50)	0
	R6	849.16668(50)	19
	R7	851.37325(50)	5
	R8	853.54035(50)	1
	R9	855.66776(50)	9
	R11	859.80190(50)	−5
	R12	861.80857(50)	14
	R13	863.77432(50)	15
	R14	865.69880(50)	−13
	R15	867.58258(50)	10
	R16	869.42471(50)	9
	R17	871.22522(50)	9
	R18	872.98382(50)	4
	R19	874.70051(50)	14
	R20	876.37479(50)	9
	R21	878.00655(50)	0
	R22	879.59579(50)	6
	R24	882.64532(50)	3
	R25	884.10528(50)	−1
	R26	885.52187(50)	2
	R27	886.89474(50)	−5
	R28	888.22390(50)	−3
	R29	889.50909(50)	−1
	R30	890.75008(50)	−4
	R31	891.94677(50)	−6
	R32	893.09916(50)	10
	R33	894.20679(50)	13
	R34	895.26944(50)	−2
	R35	896.28763(50)	31
	R36	897.26012(50)	3
	R37	898.18763(50)	1
	R38	899.07002(50)	25
	R39	899.90634(50)	−7
	R40	900.69714(50)	−26
	R41	901.44250(50)	−12
	R42	902.14189(50)	−5
	R43	902.79536(50)	11
	R44	903.40252(50)	9
	R45	903.96352(50)	16
	R46	903.47840(50)	45
	R47	904.94617(50)	9
	R48	905.36761(50)	−6
	R49	905.74250(50)	−12
	R50	906.07049(50)	−35
	R51	906.35198(50)	−27
	R55	907.00830(50)	7
$v = 6 \rightarrow 5$	P56	631.26624(50)	0
	P54	639.29894(100)	−76
	P52	647.25691(50)	−39
	P51	651.20753(100)	85
	P50	655.13622(50)	30
	P49	659.04535(100)	71
	P46	670.64369(50)	−18
	P45	674.46635(50)	−35
	P44	678.26686(50)	−25
	P43	682.04524(50)	51
	P42	685.79951(50)	32
	P41	689.53022(50)	9
	P40	693.23728(50)	12
	P39	696.91967(50)	−27
	P38	700.57774(50)	−35
	P37	704.21097(50)	−29
	P36	707.81909(50)	1
	P35	711.40128(50)	7
	P34	714.95743(50)	14
	P33	718.48678(50)	−18
	P32	721.99000(50)	11
	P31	725.46568(50)	−3
	P30	728.91460(50)	51
	P29	732.33460(50)	−9
	P28	735.72725(50)	9
	P27	739.09118(50)	1
	P26	742.42629(50)	−8
	P25	745.73224(50)	−21
	P23	752.25605(50)	17
	P22	755.47261(50)	3
	P20	761.81424(50)	−10
	P19	764.93689(200)	−187
	P18	768.03182(50)	5
	P17	771.09320(50)	12
	P16	774.12229(50)	−7
	P15	777.11933(50)	2
	P13	783.01522(50)	24
	P12	785.91301(50)	−9
	P11	788.77891(150)	124
	P10	791.60833(50)	−8
	P9	794.40495(50)	−6
	P8	797.16733(50)	15
	P7	799.89493(50)	28
	P6	802.58730(50)	19
	P5	805.24087(350)	−342
	P4	807.86617(50)	26
	P2	813.00221(100)	87
	R2	825.19847(50)	−3
	R3	827.52599(50)	14
	R4	829.81527(50)	2
	R5	832.06651(50)	8
	R6	834.27886(50)	−30
	R8	838.58819(50)	−5
	R9	840.68389(50)	−23
	R10	842.74058(50)	1
	R11	844.75707(50)	−30

TABLE 1 (*continued*)

	J''	Obs./cm^{-1}	Obs. − calc. /10^{-5} cm^{-1}
	R12	846.72833(600)	−594
	R13	848.67116(50)	10
	R14	850.56750(50)	0
	R15	852.42330(50)	−9
	R16	854.23959(50)	10
	R17	856.01250(50)	−11
	R18	857.75264(700)	712
	R19	859.43674(50)	−27
	R20	861.08708(50)	18
	R21	862.69487(50)	−9
	R22	864.26104(50)	2
	R23	865.78496(50)	10
	R24	867.26622(50)	−9
	R25	868.70521(50)	3
	R26	870.10125(50)	−3
	R27	871.45421(50)	−22
	R28	872.76452(50)	6
	R29	874.03130(50)	10
	R30	875.25442(50)	−6
	R31	876.43369(50)	−44
	R32	877.56817(200)	−183
	R33	878.66191(50)	−1
	R34	879.70976(50)	2
	R35	880.71316(50)	−16
	R36	881.67234(50)	−17
	R37	882.58714(50)	−3
	R38	883.45736(50)	20
	R39	884.28195(50)	−40
	R40	885.06264(50)	4
	R41	885.79740(50)	−41
	R42	886.48648(150)	−136
	R44	887.73275(100)	85
	R45	888.28561(50)	−12
	R47	889.25732(100)	89
	R50	890.36885(50)	14
	R51	890.64793(50)	48
	R54	891.20663(50)	8
$v = 7 \rightarrow 6$	P49	647.14517(100)	−58
	P48	650.97177(50)	−19
	P47	654.77918(200)	187
	P46	658.56125(50)	−20
	P45	662.32515(100)	116
	P44	666.06510(100)	54
	P42	673.47846(50)	12
	P41	677.15168(100)	88
	P40	680.79849(150)	−134
	P39	684.42469(50)	−38
	P38	688.02566(50)	−50
	P37	691.60208(100)	−66
	P36	695.15490(50)	45
	P35	698.68078(50)	−17
	P34	702.17991(200)	−197
	P33	705.65682(50)	−8
	P32	709.10513(50)	−52
	P31	712.51815(1000)	−965
	P30	715.92281(50)	−19
	P29	719.29063(50)	−29
	P28	722.63170(50)	49
	P27	725.94266(100)	−89
	P26	729.23121(350)	362
	P25	732.48296(50)	−5
	P24	735.70932(50)	−17
	P23	738.90654(50)	−15
	P22	742.07481(50)	52
	P21	745.21175(50)	−23
	P20	748.31931(50)	−12
	P19	751.39546(100)	−86
	P18	754.44228(50)	−7
	P17	757.44812(1000)	−908
	P16	760.44010(50)	−47
	P15	763.39169(50)	−45
	P14	766.31080(100)	−82
	P13	769.19877(50)	7
	P12	772.05255(50)	−53
	P11	774.87448(50)	1
	P10	777.66275(50)	17
	P9	780.41688(50)	−23
	P8	783.13355(500)	−423
	P7	785.82366(100)	−63
	R0	806.05185(200)	−178
	R3	813.04233(100)	−76
	R6	819.69328(300)	−302
	R7	821.83811(50)	−6
	R9	826.00653(50)	−11
	R10	828.03300(50)	22
	R11	830.02000(50)	13
	R12	831.96699(100)	−71
	R13	833.87574(50)	−29
	R14	835.74396(50)	−69
	R15	837.57308(50)	−26
	R16	839.36132(100)	−56
	R17	841.10989(50)	−18
	R18	842.81765(50)	−3
	R19	844.48452(50)	−1
	R20	846.11019(50)	−22
	R21	847.69396(150)	−116
	R22	849.23796(50)	−51
	R23	850.74056(50)	29
	R24	852.20033(50)	1
	R25	853.61839(50)	−6
	R26	854.99312(150)	−136
	R27	856.33010(200)	188
	R28	857.62348(400)	396
	R29	858.86836(50)	17
	R30	860.07412(50)	5
	R31	861.23685(50)	−16
	R33	863.43413(100)	72
	R34	864.46643(50)	−14
	R35	865.45592(50)	−25
	R36	866.40256(50)	49
	R37	867.30403(50)	−11
	R38	868.16397(200)	173
	R39	868.97640(50)	16
	R40	869.74394(250)	−208
	R41	870.47184(50)	40
	R42	871.15340(100)	100
	R43	871.78846(50)	−32
	R44	872.38031(50)	−17
	R46	873.42902(50)	−37
	R49	874.66493(50)	−19
$v = 8 \rightarrow 7$	P42	661.42085(150)	141
	P38	675.74003(50)	10
	P35	686.23006(100)	98
	P33	693.09693(50)	−3
	P32	696.49270(50)	31
	P30	703.20429(50)	−28
	P28	709.80945(50)	−11
	P27	713.07091(50)	−12

TABLE 1 (*continued*)

	J''	Obs./cm^{-1}	Obs. − calc. /10^{-5} cm^{-1}
	P26	716.30457(50)	−14
	P25	719.51041(50)	14
	P24	722.68777(50)	38
	P23	725.83593(50)	19
	P22	728.95561(50)	61
	P21	732.04517(50)	30
	P20	735.10512(50)	11
	P19	738.13524(50)	12
	P18	741.13479(50)	−10
	P17	744.10391(50)	−10
	P15	749.95028(150)	121
	P14	752.82567(150)	126
	R3	798.85770(150)	142
	R4	801.07990(150)	160
	R8	809.60458(1000)	1080
	R9	811.62911(100)	81
	R10	813.62541(100)	79
	R13	819.37905(300)	−305
	R14	821.22278(100)	−59
	R15	823.02561(50)	29
	R19	829.83516(100)	−69
	R25	838.83764(50)	−28
	R27	841.50984(100)	91
	R28	842.78178(50)	−6
	R29	844.01424(150)	146
	R30	845.20204(50)	44
	R31	846.34856(50)	42
	R32	847.45203(50)	−21
	R34	849.53230(50)	−24
	R37	852.33205(100)	97
	R38	853.17689(100)	−64
^{6}LiF $v = 1 \rightarrow 0$	P49	751.39546(200)	174
	P48	756.18469(100)	−82
	P47	760.94616(500)	−442
	P46	765.68855(50)	13
	P45	770.39839(50)	−14
	P44	775.08005(50)	−37
	P43	779.73328(50)	−30
	P42	784.35734(50)	−19
	P41	788.95138(50)	−40
	P40	793.51789(250)	206
	P38	802.55164(50)	21
	P37	807.02133(100)	−68
	P36	811.46031(50)	−19
	P35	815.86652(50)	12
	P34	820.23918(50)	−8
	P33	824.57866(50)	5
	P32	828.88382(50)	−17
	P31	833.15515(50)	22
	P30	837.39117(50)	18
	P29	841.59199(50)	28
	P28	845.75658(50)	−6
	P27	849.88539(50)	5
	P26	853.97776(50)	40
	P25	858.03243(50)	16
	P24	862.04978(50)	17
	P23	866.02906(50)	8
	P22	869.96988(50)	−4
	P21	873.87216(50)	15
	P19	881.55813(50)	15
	P18	885.34109(50)	9
	P17	889.08367(50)	16
	P16	892.78527(500	20
	P15	896.44556(50)	26
	P14	900.06386(50)	8
	P13	903.64038(50)	27
	P12	907.17407(50)	17
	P11	910.66485(50)	11
	P9	917.51612(50)	8
	P8	920.87587(50)	14
	P6	927.46149(50)	22
	P5	930.68665(50)	29
	P4	933.86603(50)	18
	P3	936.99984(50)	47
	P2	940.08696(50)	42
	R1	951.96648(200)	178
	R2	954.81511(50)	26
	R3	957.61714(50)	58
	R4	960.36968(50)	19
	R5	963.07337(50)	7
	R7	968.33239(50)	14
	R8	970.88707(50)	32
	R9	973.39100(50)	16
	R10	975.84433(50)	13
	R11	978.24675(50)	23
	R12	980.59770(50)	20
	R13	982.89712(50)	29
	R14	985.14439(50)	17
	R15	987.33946(50)	9
	R16	989.48225(50)	25
	R17	991.57200(50)	18
	R18	993.60879(50)	25
	R19	995.59199(50)	9
	R20	997.52168(50)	7
	R21	999.39761(50)	19
	R22	1001.21912(50)	6
	R23	1002.98612(50)	−15
	R24	1004.69906(50)	27
	R25	1006.35654(50)	15
	R26	1007.95899(50)	18
	R27	1009.50605(50)	24
	R28	1010.99719(50)	2
	R29	1012.43284(50)	19
	R30	1013.81195(50)	−7
	R31	1015.13504(50)	−3
	R32	1016.40130(50)	−28
	R33	1017.61128(50)	−7
	R34	1018.76427(50)	11
	R35	1019.85968(50)	−14
	R36	1020.89828(50)	14
	R37	1021.87841(50)	−52
	R38	1022.80178(50)	−22
	R39	1023.66705(50)	−13
	R40	1024.47393(50)	−36
	R41	1025.22300(50)	−17
	R42	1025.91354(50)	−12
	R43	1026.54473(100)	−88
	R44	1027.11936(100)	50
	R45	1027.63336(50)	9
	R46	1028.08907(50)	36
	R47	1028.48432(50)	−72
	R48	1028.82102(100)	−113
	R49	1029.09819(150)	−171
	R50	1029.31757(50)	−62
	R51	1029.47703(50)	11
	R52	1029.57530(50)	−67
$v = 2 \rightarrow 1$	P45	755.43538(100)	−67

TABLE 1 (*continued*)

	J''	Obs./cm^{-1}	Obs. − calc. /10^{-5} cm^{-1}
	P43	764.61478(50)	−45
	P41	773.67949(50)	−60
	P40	778.16834(50)	−10
	P39	782.62662(50)	−13
	P38	787.05450(50)	−6
	P37	791.45148(50)	9
	P36	795.81657(50)	−19
	P35	800.14984(50)	−37
	P34	804.45136(50)	8
	P33	808.71805(150)	−145
	P32	812.95455(50)	13
	P31	817.15543(50)	−15
	P30	821.32216(50)	−37
	P29	825.45465(50)	−16
	P28	829.55201(50)	3
	P27	833.61364(50)	3
	P26	837.63928(50)	4
	P25	841.62865(50)	20
	P24	845.58079(50)	0
	P23	849.49399(200)	−185
	P21	857.21231(50)	−5
	P20	861.01304(50)	5
	P19	864.77476(50)	13
	P18	868.49715(50)	28
	P17	872.17929(50)	−2
	P16	875.82136(50)	−17
	P15	879.42319(50)	6
	P14	882.98366(50)	−4
	P13	886.50302(50)	16
	P12	889.98011(50)	−9
	P11	893.41533(50)	0
	P9	900.15735(50)	−7
	P8	903.46399(50)	37
	P7	906.72608(50)	0
	P6	909.94425(50)	−18
	P5	913.11846(50)	17
	P4	916.24665(100)	−66
	P3	919.33092(50)	−18
	R1	934.05897(50)	−45
	R2	936.86533(100)	83
	R3	939.62222(50)	29
	R4	942.33100(50)	−36
	R6	947.60494(50)	−1
	R7	950.16843(50)	−2
	R8	952.68273(50)	7
	R9	955.14718(50)	−9
	R10	957.56191(50)	−6
	R11	959.92643(50)	−2
	R12	962.24050(50)	8
	R13	964.50353(50)	−3
	R14	966.71581(50)	21
	R15	968.87667(50)	44
	R16	970.98505(50)	−13
	R17	973.04232(50)	15
	R18	975.04697(50)	6
	R19	976.99921(50)	8
	R20	978.89871(50)	13
	R21	980.84527(50)	29
	R22	982.53819(50)	11
	R23	984.27761(50)	−2
	R24	985.96322(50)	−14
	R25	987.59499(50)	−6
	R26	989.17244(50)	−2
	R27	990.69572(50)	39
	R28	992.16338(50)	−8
	R29	993.57652(50)	−9
	R30	994.93450(50)	−6
	R31	996.23725(50)	15
	R32	997.48431(50)	29
	R33	998.67506(50)	−5
	R34	999.81007(50)	−11
	R35	1000.88915(50)	12
	R36	1001.91146(50)	−1
	R37	1002.87728(50)	−5
	R38	1003.78611(50)	−30
	R39	1004.63850(50)	−5
	R40	1005.43360(50)	1
	R41	1006.17163(50)	27
	R42	1006.85155(50)	−16
	R43	1007.47425(50)	−24
	R44	1008.03932(50)	−23
	R45	1008.54547(150)	−129
	R46	1008.99703(150)	105
	R47	1009.38662(50)	−47
	R48	1009.71917(50)	−80
$v = 3\rightarrow 2$	P41	758.75890(100)	99
	P40	763.17149(50)	−22
	P38	771.91079(50)	14
	P37	776.23471(50)	−13
	P36	780.52789(50)	−33
	P34	789.02044(50)	−25
	P33	793.21835(50)	−52
	P32	797.38225(250)	−214
	P31	801.51430(250)	−252
	P30	805.61544(50)	−25
	P29	809.68058(50)	1
	P28	813.71070(50)	−31
	P27	817.70707(50)	50
	P26	821.66970(300)	289
	P25	825.59133(50)	2
	P24	829.47955(50)	−7
	P22	837.14646(50)	45
	P21	840.92343(50)	19
	P19	848.36390(50)	22
	P18	852.02613(50)	7
	P17	855.64945(50)	11
	P16	859.23324(50)	13
	P15	862.77709(50)	11
	P14	866.28072(50)	19
	P13	869.74394(50)	55
	P12	873.16500(50)	−15
	P11	876.54562(50)	19
	P9	883.18000(50)	−2
	P8	886.43358(50)	1
	P7	889.64414(50)	3
	P6	892.81130(50)	1
	P5	895.93473(50)	0
	P4	899.01544(150)	136
	P2	905.04087(200)	184
	R3	922.01884(50)	5
	R4	924.68524(50)	−24
	R5	927.30477(50)	14
	R7	932.39898(50)	−8
	R8	934.87365(50)	−5
	R9	937.29833(150)	−121
	R10	939.67647(50)	19
	R11	942.00368(50)	7
	R12	944.28135(50)	11

TABLE 1 (*concluded*)

J''	Obs./cm^{-1}	Obs. − calc. /10^{-5} cm^{-1}	J''	Obs./cm^{-1}	Obs. − calc. /10^{-5} cm^{-1}
R13	946.50882(50)	−5	R28	973.73717(50)	−32
R14	948.68641(50)	19	R29	975.12887(50)	2
R15	950.81344(50)	45	R30	976.46613(50)	22
R16	952.88892(50)	0	R31	977.74904(100)	58
R17	954.91365(50)	−6	R32	978.97634(50)	4
R18	956.88709(50)	−2	R33	980.14903(50)	−19
R19	958.80858(50)	−26	R34	981.26726(50)	22
R20	960.67877(50)	14	R35	982.32871(100)	−85
R21	962.49611(50)	−13	R36	983.33625(50)	−34
R22	964.26116(50)	−24	R38	985.18360(50)	9
R23	965.97345(50)	−43	R39	986.02215(100)	−91
R24	967.63365(50)	23	R40	986.80581(50)	−63
R25	969.23974(50)	−4	R41	987.53253(100)	−98
R26	970.79251(50)	−22	R43	988.81787(50)	−23
R27	972.29165(50)	−39			

[a]Numbers in parentheses are estimated uncertainties.

sities of the emission lines increased with higher temperature. The maximum temperature which is accessible with our current system is about 1500 K and it was at this temperature that the best emission spectrum was obtained. All emission signals decreased rapidly as the furnace cooled and disappeared at about 1200 K.

III. Results

The emission features were observed in the region where the infrared spectrum of MgF_2 was expected (Figs. 1, 2). However, the high resolution spectrum showed a pattern typical of a diatomic molecule. After some thought and a literature search we found that the emission spectrum belonged to LiF (11). The presence of Li in our system was puzzling but in a previous experiment the alumina tube was used to vaporize LiNC. Despite careful cleaning of the cell, some Li remained on the walls of the alumina tube. At higher temperatures the MgF_2 could react with water (which is always present in the system) and form HF. The HF can react with the Li impurities and produce LiF. Direct reduction of MgF_2 with Li is also possible but MgF was not detected. An additional reaction of HF with the alumina tube took place to form AlF. The emission of AlF was observed in the spectrum (17).

The spectral analysis program PC-DECOMP, developed by J. W. Brault, was used for data analysis. The rotational line profiles were fit to Voigt lineshape functions. The strong lines show a "ringing" caused by the (sin x/x) lineshape function of the Fourier transform spectrometer. The ringing was eliminated by using the "filter fitting" routine available in PC-DECOMP. The signal-to-noise ratio for the strong lines was better than 1000 and the resulting resolution-enhanced line width was 0.0005 cm^{-1}. The HF lines were used for absolute calibration (+/−0.0002 cm^{-1}) of the spectrum. For this calibration the HF absorption lines, taken in a spectrum at lower temperature, were calibrated against CO_2 (18).

The assignment of the vibrational bands of the main isotopomer ^{7}LiF was straightforward (Table 1). Data reduction was made by using Dunham's equation (19)

$$[1]\quad T(v,J) = \sum_{i,j} Y_{ij}\left(v+\frac{1}{2}\right)^i [J(J+1)]^j$$

Pure rotational transitions reported by Pearson and Gordy (20) were included in the fit. The Dunham coefficients obtained from this fit are shown in Table 2.

TABLE 2. Dunham constants for LiF (in cm^{-1})[a]

Constant	Value ^{7}LiF	^{6}LiF
Y_{10}	910.57272(10)	964.30621(22)
Y_{20}	−8.207956(46)	−9.19819(12)
Y_{30}	0.569166(82)	0.64808(20)
Y_{40}	−0.28437(49)E−3	
Y_{01}	1.34525715(57)	1.5087385(14)
Y_{11}	−0.02028749(19)	−0.02409773(41)
Y_{21}	0.156247(64)E−3	0.19766(15)E−3
Y_{31}	−0.3860(88)E−6	−0.736(21)E−6
Y_{41}	−0.870(45)E−8	
Y_{02}	−0.1174389(33)E−4	−0.147719(13)E−4
Y_{12}	0.113878(98)E−6	0.15246(29)E−6
Y_{22}	0.720(23)E−9	0.619(33)E−9
Y_{32}	−0.306(13)E−10	
Y_{03}	0.30449(55)E−10	0.4300(35)E−10
Y_{13}	0.836(15)E−12	0.1120(70)E−11
Y_{23}	−0.270(27)E−13	

[a]Each isotopomer was fit independently. One standard deviation in parentheses.

The assignment of the vibrational bands of the minor isotopomer, ^{6}LiF, was carried out by comparing predicted line positions with the unassigned lines in the spectrum. The line positions for ^{6}LiF are also shown in Table 1. The mass-dependent Dunham coefficients Y_{ij} are listed in Table 2.

Finally, all infrared and microwave data for LiF was combined and fit to the mass-reduced Dunham expression including Watson's correction due to the breakdown of the Born–Oppenheimer approximation (21, 22)

$$[2]\quad Y_{ij} = \mu^{[(i+2j)/2]} U_{ij}\left[1+\left(\frac{m_e}{m_{Li}}\right)\Delta_{ij}\right]$$

where μ is the reduced mass, U_{ij} are the mass-independent parameters, m_{Li} is the atomic mass of Li (23), m_e is the electron mass, and Δ_{ij} is the mass scaling factor for the Li atom. The

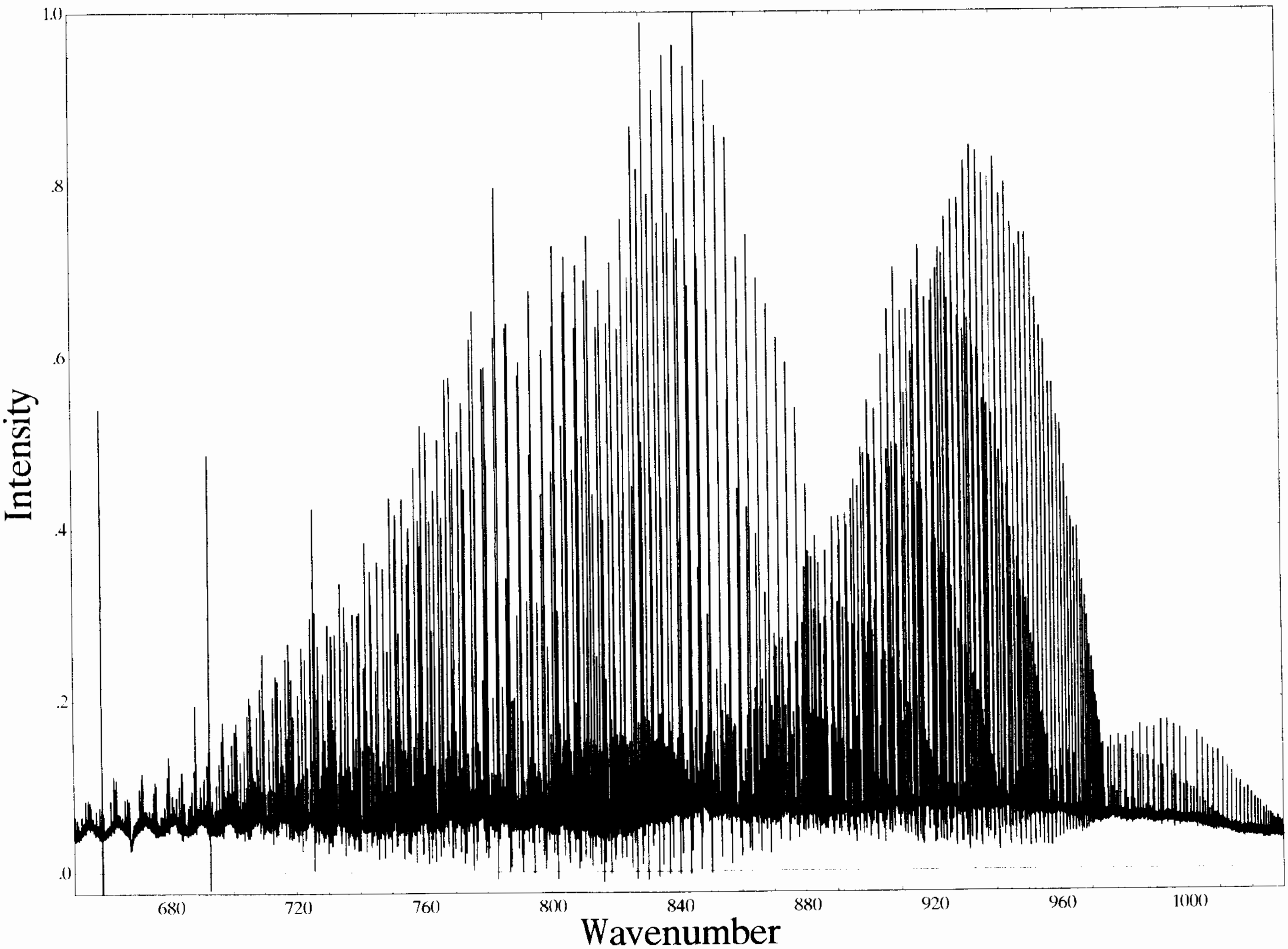

FIG. 1. Infrared spectrum of ^{7}LiF.

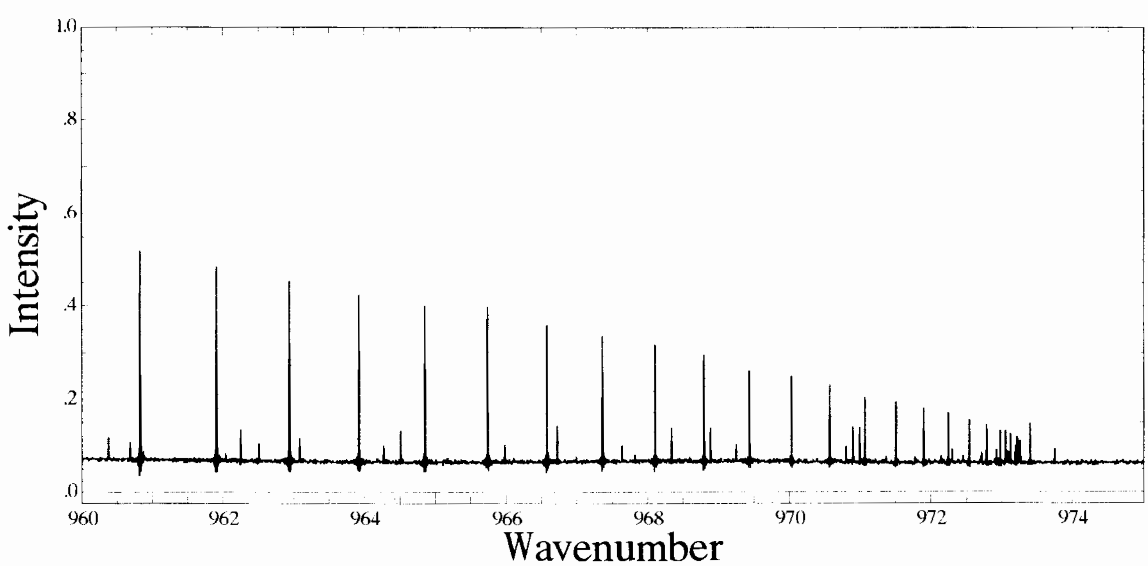

FIG. 2. Infrared spectrum of ^{6}LiF.

TABLE 3. Mass-reduced Dunham constants for LiF (in cm^{-1})[a]

Constant	Our work
U_{10}	2061.15184(33)
U_{20}	−42.05641(19)
U_{30}	0.660241(80)
U_{40}	−7.480(11)E−3
U_{01}	6.8926542(36)
U_{11}	−0.2352993(16)
U_{21}	4.1016(14)E−3
U_{31}	−0.2259(44)E−4
U_{41}	−0.1199(52)E−5
U_{02}	−0.3083223(30)E−3
U_{12}	0.67650(42)E−5
U_{22}	0.991(25)E−7
U_{32}	−0.995(32)E−8
U_{03}	0.40964(30)E−8
U_{13}	0.2566(34)E−9
U_{23}	−0.186(17)E−10
Δ_{10}	0.0417(17)
Δ_{01}	0.3595(58)

[a]One standard deviation in parentheses.

TABLE 4. Pure rotational transitions of HF

J'	J''	Observed/cm^{-1}	Obs. − calc. /10^{-5} cm^{-1}	Uncertainty (1σ) /10^{-5} cm^{-1}
1	0	41.1109832[a]	0.181	0.15
2	1	82.1711179[a]	0.139	0.3
3	2	123.12967[a]	−1	0.5
4	3	163.93616[a]	0	0.5
5	4	204.54045[b]	1	10
6	5	244.89283[b]	0	10
7	6	284.94444[b]	23	15
13	12	516.28061[c]	−14	20
14	13	552.92046[c]	9	20
15	14	588.89904[c]	−1	20
16	15	624.17733[c]	11	20
17	16	658.71682[c]	4	20
18	17	692.48121[c]	8	20
19	18	725.43557[c]	38	20
20	19	757.54540[c]	−13	20
21	20	788.78013[c]	−15	20
22	21	819.10918[c]	−8	20
23	22	848.50386[c]	−8	20
24	23	876.93745[c]	−5	20
25	24	904.38481[c]	5	20
27	26	956.22816[d]	−3	13
28	27	980.5832[e]	74	75
29	28	1003.8672[e]	62	50
31	30	1047.1570[e]	−169	125
32	31	1067.1377[e]	−11	50
33	32	1085.98903[d]	0	13

[a]Tunable far infrared spectroscopy (ref. 12).
[b]Fourier transform spectroscopy (ref. 12).
[c]Fourier transform spectroscopy (our work).
[d]Diode laser heterodyne spectroscopy (ref. 14).
[e]Diode laser spectroscopy (ref. 12).

TABLE 5. Rotational constants of ground state HF[a]

Constant	Our work /cm^{-1}	Jennings *et al.* (12) /cm^{-1}
B_0	20.5597298(8)	20.5597300(25)
D_0	2.119901(36)E−3	2.11991(14)E−3
H_0	0.163483(116)E−6	0.16334(50)E−6
L_0	−0.14974(132)E−10	−0.1473(66)E−10
M_0	0.1052(50)E−14	0.94(27)E−15

[a]Two standard deviations in parentheses.

data required two Δ's, one for U_{10} ("ω_e") and one for U_{01} ("B_e"). The final mass-independent coefficients and the Δ's are listed in Table 3.

The energy levels of HF were fit to the expression (24)

$$[3] \quad E_v(J) = B_vJ(J+1) - D_v[J(J+1)]^2 + H_v[J(J+1)]^3 + L_v[J(J+1)]^4 + M_v[J(J+1)]^5$$

The fit includes all lines listed in Table 4 and Table 5 shows the determined constants.

IV. Conclusion

The high-resolution infrared emission spectra of LiF and HF were observed with a Fourier transform instrument. The ro-vibrational transitions of the fundamental band and of seven hot bands for ^{7}LiF and of three bands for ^{6}LiF were rotationally analyzed. Pure rotational transitions for HF were also observed and enabled us to calculate an improved set of molecular constants. The accuracy of the line positions allows the use of HF as an absolute wavenumber standard.

Acknowledgements

The National Solar Observatory is operated by the Association of Universities for Research in Astronomy, Inc., under the contract with the National Science Foundation. We would like to thank J. W. Brault and J. Wagner for assistance in recording the spectra. This work was supported by the Astronautics Laboratory, Edwards Air Force Base, CA. Acknowledgement is made to the Petroleum Research Fund, administered by the American Chemical Society, for partial support of this work. One of us (H.G.H.) thanks the Deutsche Forschungsgemeinschaft for a postdoctoral scholarship.

1. S. E. VEAZEY and W. GORDY. Phys. Rev. A, **138**, 1303 (1965).
2. A. J. HEBERT, F. J. LOVAS, C. A. MELENDRES, C. D. HOLLOWELL, T. L. STORY, JR., and K. STREET, JR. J. Chem. Phys. **48**, 2824 (1968).
3. G. L. VIDALE. J. Phys. Chem. **64**, 314 (1960).
4. L. WHARTON, W. KLEMPERER, L. P. GOLD, R. STRAUCH, J. J. GALLAGHER, and V. E. DERR. J. Chem. Phys. **38**, 1203 (1963).
5. M. J. LINEVSKY. J. Chem. Phys. **34**, 587 (1961).
6. M. J. LINEVSKY. J. Chem. Phys. **38**, 658 (1963).
7. A. SNELSON and K. S. PITZER. J. Phys. Chem. **67**, 882 (1963).
8. S. SCHLICK and O. SCHNEPP. J. Chem. Phys. **41**, 463 (1964).
9. A. SNELSON. J. Chem. Phys. **46**, 3652 (1967).
10. S. ABRAMOWITZ, N. ACQUISTA, and I. W. LEVIN. J. Res. Nat. Bur. Stand. Sect. A, **72**, 487 (1968).
11. A. MAKI. J. Mol. Spectrosc. **102**, 361 (1983).
12. D. A. JENNINGS, K. M. EVENSON, L. R. ZINK, C. DEMUYNCK, J. L. DESTOMBES, B. LEMOINE, and J. W. C. JOHNS. J. Mol. Spectrosc. **122**, 477 (1987).

13. U. K. SENGUPTA, P. K. DAS, and K. N. RAO. J. Mol. Spectrosc. **74**, 322 (1979).
14. D. A. JENNINGS and J. S. WELLS. J. Mol. Spectrosc. **130**, 267 (1988).
15. J. S. WELLS, F. R. PETERSON, A. G. MAKI, and D. J. SUKLE. Appl. Opt. **20**, 1676 (1981).
16. C. I. FRUM, R. ENGLEMAN, JR., and P. F. BERNATH. J. Chem. Phys. **93**, 5457 (1990).
17. H. G. HEDDERICH, C. I. FRUM, R. ENGLEMAN, JR., and P. F. BERNATH. To be published.
18. G. GUELACHVILI and K. N. RAO. Handbook of infrared standards. Academic Press, Orlando, FL. 1986.
19. J. L. DUNHAM. Phys. Rev. **41**, 721 (1932).
20. E. F. PEARSON and W. GORDY. Phys. Rev. **177**, 52 (1969).
21. J. K. G. WATSON. J. Mol. Spectrosc. **45**, 99 (1973).
22. J. K. G. WATSON. J. Mol. Spectrosc. **80**, 411 (1980).
23. H. S. PEISER, N. E. HOLDEN, P. DE BIEVRE, I. L. BARNES, R. HAGEMANN, J. R. DE LAETER, T. J. MURPHY, E. ROTH, M. SHIMA, and H. G. THODE. Pure Appl. Chem. **56**, 695 (1984).
24. W. GORDY and R. L. COOK. Microwave molecular spectra. Wiley, New York, NY. 1984.